universe

MDPI

Article

Study of Decoupled Anisotropic Solutions in $f(R, T, R_{\rho\eta}T^{\rho\eta})$ Theory

Tayyab Naseer and Muhammad Sharif *

Department of Mathematics, Quaid-e-Azam Campus, University of the Punjab, Lahore 54590, Pakistan; tayyabnaseer48@yahoo.com

* Correspondence: msharif.math@pu.edu.pk

Abstract: In this paper, we consider isotropic solution and extend it to two different exact well-behaved spherical anisotropic solutions through minimal geometric deformation method in $f(R, T, R_{\rho\eta}T^{\rho\eta})$ gravity. We only deform the radial metric component that separates the field equations into two sets corresponding to their original sources. The first set corresponds to perfect matter distribution while the other set exhibits the effects of additional source, i.e., anisotropy. The isotropic system is resolved by assuming the metric potentials proposed by Krori-Barua while the second set needs one constraint to be solved. The physical acceptability and consistency of the obtained solutions are analyzed through graphical analysis of effective matter components and energy bounds. We also examine mass, surface redshift and compactness of the resulting solutions. For particular values of the decoupling parameter, our both solutions turn out to be viable and stable. We conclude that this curvature-matter coupling gravity provides more stable solutions corresponding to a self-gravitating geometry.

Keywords: $f(R, T, R_{\rho\eta}T^{\rho\eta})$ gravity; anisotropy; gravitational decoupling; self-gravitating systems

PACS: 04.50.Kd; 04.40.Dg; 04.40.-b

Citation: Naseer, T.; Sharif, M. Study of Decoupled Anisotropic Solutions in $f(R, T, R_{\rho\eta}T^{\rho\eta})$ Theory. *Universe* **2022**, *8*, 62. https://doi.org/10.3390/universe8020062

Academic Editors: Mariusz P. Dąbrowski, Adam Balcerzak and Vincenzo Salzano

Received: 6 December 2021
Accepted: 7 January 2022
Published: 19 January 2022

1. Introduction

Einstein theory of general relativity (GR) has been considered as the root of cosmology and gravitational phenomena. Cosmological findings show that the astronomical objects are not scattered randomly in the universe but are organized in a systematic way. The investigation of this arrangement and physical characteristics of interstellar bodies enable us to figure out accelerated expansion of the cosmos. This expansion is presumed to be performed by an obscure form of energy known as dark energy. Moreover, the virial mass discrepancy at the galactic cluster level and the galaxy rotation curves [1,2], cosmic accelerated expansion as well as other cosmological observations suggest that the standard general relativistic gravitational field equations, based on the Einstein-Hilbert (EH) action cannot describe the universe at large scales. From cosmological point of view, dark matter and dark energy components are introduced by hand, in addition to ordinary matter and energy in this theory. The modifications to GR are found to be crucial in unveiling mysterious aspects of our universe. The $f(R)$ theory is the immediate extension of GR, formulated on the basis of an arbitrary function that replaces the Ricci scalar R in the EH action. The stability of $f(R)$ theory has been discussed by various researchers by using different approaches [3–5]. Capozziello et al. [6] studied the stability of different stars in $f(R)$ theory by utilizing the Lané-Emden equation. Recently, various experiments have been conducted on the astronomical objects to discuss their composition and stability in this theory [7–12].

Later, Bertolami et al. [13] considered the Lagrangian depending on scalar curvature R and $\mathcal{L}_m$ to study the effects of coupling in $f(R)$ gravity. The coupling between matter and spacetime in extended theories of GR has encouraged several theorists to focus on cosmic

accelerated expansion. Harko et al. [14] proposed $f(R,T)$ theory to study the non-minimal interaction between matter and geometry, T represents trace of the energy-momentum tensor (EMT). It has been observed that such a coupling results in the non-conservation of EMT which may cause the accelerated interstellar expansion. Haghani et al. [15] presented a wider and more complex theory by adding an extra term in the Lagrangian of $f(R,T)$ theory to study the strong effects of non-minimal coupling, referred to $f(R,T,Q)$ theory, in which $Q \equiv R_{\rho\eta}T^{\rho\eta}$. Indeed, examples of such couplings can be found in the Einstein-Born-Infeld theories when one expands the square root in the Lagrangian. In this framework, Sharif and Zubair investigated the energy bounds for some particular models [16] and checked the feasibility of thermodynamical laws [17].

This theory was constructed on the basis of insertion of the strong non-minimal matter-geometry coupling which is explained by the factor Q. The role of dark matter and dark energy, without resorting to exotic matter distribution is explained through the modification in the EH action. Several extended theories such as $f(R,\mathcal{L}_m)$ and $f(R,T)$ also engage such arbitrary coupling but their functionals cannot be considered in the most general form to understand the effects of coupling on celestial objects in some situations. It should be pointed out that the factor $R_{\rho\eta}T^{\rho\eta}$ could interpret non-minimal interaction in the scenario where $f(R,T)$ theory fails to describe. In particular, one cannot explain coupling effects on the gravitational model in $f(R,T)$ theory when trace-free EMT (i.e., $T=0$) is considered, while $f(R,T,Q)$ gravity studies such effects even in this context. This theory was shown to be stable against Dolgov-Kawasaki instability and can help to explain the galactic rotation curves due to the presence of an additional force which stops the motion of test particles in geodesic path. Haghani et al. [15] discussed cosmological applications of three different models in this framework, i.e., $R+\alpha Q$, $R(1+\alpha Q)$ and $R+\beta\sqrt{\mid T \mid}+\alpha Q$, where α and β are arbitrary coupling constants. They analyzed the evolution and dynamics of the universe for the above models with and without energy conservation.

Odintsov and Sáez-Gómez [18] found some analytical as well as numerical solutions in $f(R,T,Q)$ theory and compared them with the ΛCDM model. They also discussed some problems related to the instability of fluid distribution. Ayuso et al. [19] inspected the consistency and reliability of this complicated theory by choosing some suitable scalar (or vector) fields. Baffou et al. [20] explored the power-law solution to understand the early cosmic evolution and checked the stability for some specific models. Sharif and Waseem [21,22] studied certain physical attributes of massive isotropic/anisotropic configured stars and checked their stable regions. Yousaf et al. [23–27] computed several structure scalars for static and non-static cases which are related with the fundamental properties of matter distribution. These scalars help to illustrate the composition and expansion of self-gravitating stellar configuration.

Owing to the inclusion of highly non-linear terms in the field equations of a compact geometry, the development of exact solutions has always been a serious but interesting issue. Gravitational decoupling is a recently proposed scheme which is used to find feasible solutions corresponding to the matter distribution involving multiple sources, such as anisotropy, heat dissipation and shear stress. The minimal geometric deformation (MGD) technique has shown significant consequences to achieve physically well-behaved solutions. This approach offers a variety of enticing ingredients for new exact solutions for both cosmology and astrophysics. Ovalle [28] initially proposed this technique to acquire analytical solutions of stellar objects in the context of braneworld. Later, Ovalle and Linares [29] found exact spherical isotropic solutions and concluded that these results are compatible with the Tolman-IV solution in the braneworld. Casadio et al. [30] formed the outer spherical solutions and noticed that these solutions contain singularity at Schwarzschild radius.

Ovalle [31] determined anisotropic solutions via gravitational decoupling approach. Ovalle et al. [32] extended the isotropic solutions through this approach and checked the graphical behavior of new solutions which contain effects of anisotropy. Sharif and Sadiq [33] developed anisotropic solutions for charged spherical geometry by taking the Krori-Barua solution and analyzed the influence of charge on their viability as well as stability. Sharif and his collaborators [34–37] generalized this work to $f(G)$ and $f(R)$ theories.

Gabbanelli et al. [38] determined different anisotropic solutions in view of the Duragpal-Fuloria isotropic spacetime and found them physically acceptable. Estrada and Tello-Ortiz [39] constructed various anisotropic physically consistent solutions by applying this technique to Heintzmann solution. By taking an appropriate deformation function, Singh et al. [40] employed embedding technique to develop anisotropic solutions via this approach. Hensh and Stuchlik [41] deformed Tolman VII solution and found physically feasible anisotropic solutions. Sharif and Majid [42–44] considered different known isotropic solutions and found anisotropic spherical solutions with the help of minimal and extended version of the decoupling scheme in Brans-Dicke theory.

This paper investigates the influence of $f(R,T,Q)$ correction terms on two anisotropic solutions obtained through MGD approach for spherical spacetime. The paper is structured as follows. The basic formulation of this gravity is presented in the following section. Section 3 discusses the MGD technique which helps to separate the gravitational field equations into two sets which correspond to isotropic and anisotropic configurations. In Section 4, we consider the Krori-Barua spacetime to find new analytic solutions. We also discuss physical feasibility of the developed anisotropic solutions. Finally, we summarize our results in the last section.

2. The $f(R,T,Q)$ Theory

The corresponding Einstein-Hilbert action is [18]

$$S=\int\frac{1}{16\pi}\left[f(R,T,R_{\rho\eta}T^{\rho\eta})+\mathcal{L}_m\right]\sqrt{-g}d^4x, \tag{1}$$

where $\mathcal{L}_m$ denotes the matter Lagrangian which in this case is considered to be negative of the energy density of fluid and g describes determinant of the metric tensor. By adding the Lagrangian $\mathcal{L}_\Theta$, which corresponds to an additional source term coupled with gravity in the action (1) and varying it with respect to the metric tensor, the field equations can be written as

$$G_{\rho\eta}=8\pi T^{(tot)}_{\rho\eta}, \tag{2}$$

where $G_{\rho\eta}$ is the Einstein tensor and the EMT for matter distribution is

$$T^{(tot)}_{\rho\eta}=T^{(eff)}_{\rho\eta}+\sigma\Theta_{\rho\eta}=\frac{1}{f_R-\mathcal{L}_m f_Q}T_{\rho\eta}+T^{(D)}_{\rho\eta}+\sigma\Theta_{\rho\eta}, \tag{3}$$

σ represents the decoupling parameter, $\Theta_{\rho\eta}$ may contain some new fields that produce anisotropic effects in self-gravitating structure. Also, we can stress $T^{(eff)}_{\rho\eta}$ as the EMT in $f(R,T,Q)$ gravity which contains usual as well as modified correction terms. In this case, the value of $T^{(D)}_{\rho\eta}$ becomes

$$\begin{aligned}T^{(D)}_{\rho\eta} &= \frac{1}{8\pi(f_R-\mathcal{L}_m f_Q)}\left[\left(f_T+\frac{1}{2}Rf_Q\right)T_{\rho\eta}+\left\{\frac{R}{2}(\frac{f}{R}-f_R)-\mathcal{L}_m f_T\right.\right.\\ &- \left.\frac{1}{2}\nabla_\pi\nabla_\beta(f_Q T^{\pi\beta})\right\}g_{\rho\eta}-\frac{1}{2}\Box(f_Q T_{\rho\eta})-(g_{\rho\eta}\Box-\nabla_\rho\nabla_\eta)f_R\\ &- \left.2f_Q R_{\pi(\rho}T^{\pi}_{\eta)}+\nabla_\pi\nabla_{(\rho}[T^{\pi}_{\eta)}f_Q]+2(f_Q R^{\pi\beta}+f_T g^{\pi\beta})\frac{\partial^2\mathcal{L}_m}{\partial g^{\rho\eta}\partial g^{\pi\beta}}\right],\end{aligned} \tag{4}$$

where $f_R=\frac{\partial f(R,T,Q)}{\partial R}$, $f_T=\frac{\partial f(R,T,Q)}{\partial T}$, $f_Q=\frac{\partial f(R,T,Q)}{\partial Q}$ and ∇_ν describes the covariant derivative. Also, $\Box\equiv g^{\rho\eta}\nabla_\rho\nabla_\eta$. The EMT for perfect fluid has the following form

$$T_{\rho\eta}=(\mu+P)u_\rho u_\eta+Pg_{\rho\eta}, \tag{5}$$

where u_ρ and P are the four-velocity and isotropic pressure, respectively. In GR, the trace of EMT provides a particular relationship between R and T. One can establish the trace of $f(R,T,Q)$ field equations as

$$3\nabla^{\eta}\nabla_{\eta}f_R + R\left(f_R - \frac{T}{2}f_Q\right) - T(f_T+1) + \frac{1}{2}\nabla^{\eta}\nabla_{\eta}(f_Q T) + \nabla_{\eta}\nabla_{\rho}(f_Q T^{\rho\eta})$$
$$- 2f + (Rf_Q + 4f_T)\mathcal{L}_m + 2R_{\rho\eta}T^{\rho\eta}f_Q - 2g^{\pi\beta}\frac{\partial^2\mathcal{L}_m}{\partial g^{\pi\beta}\partial g^{\rho\eta}}\left(f_T g^{\rho\eta} + f_Q R^{\rho\eta}\right) = 0.$$

The $f(R,T)$ gravity can be achieved from above equation by taking $Q=0$, while one can also attain $f(R)$ theory for the vacuum case.

The geometry under consideration is distinguished by a hypersurface Σ which delineates the inner and outer sectors of spherical spacetime. We define the spherical geometry which represents the interior spacetime as

$$ds^2 = -e^{\nu}dt^2 + e^{\chi}dr^2 + r^2d\theta^2 + r^2\sin^2\theta d\vartheta^2, \tag{6}$$

where $\nu = \nu(r)$ and $\chi = \chi(r)$. The corresponding four-velocity and four-vector in the radial direction are

$$u^{\rho} = (e^{\frac{-\nu}{2}}, 0, 0, 0), \quad w^{\rho} = (0, e^{\frac{-\chi}{2}}, 0, 0), \tag{7}$$

which satisfy the relations $w^{\rho}u_{\rho} = 0, u^{\rho}u_{\rho} = -1$. The field equations are

$$e^{-\chi}\left(\frac{\chi'}{r} - \frac{1}{r^2}\right) + \frac{1}{r^2} = 8\pi\left(\mu^{(eff)} - T_0^{0(D)} - \sigma\Theta_0^0\right), \tag{8}$$
$$e^{-\chi}\left(\frac{1}{r^2} + \frac{\nu'}{r}\right) - \frac{1}{r^2} = 8\pi\left(P^{(eff)} + T_1^{1(D)} + \sigma\Theta_1^1\right), \tag{9}$$
$$-\frac{e^{-\chi}}{4}\left[\chi'\nu' - \nu'^2 - 2\nu'' + \frac{2\chi'}{r} - \frac{2\nu'}{r}\right] = 8\pi\left(P^{(eff)} + T_2^{2(D)} + \sigma\Theta_2^2\right), \tag{10}$$

where $\mu^{(eff)} = \frac{1}{(f_R+\mu f_Q)}\mu$ and $P^{(eff)} = \frac{1}{(f_R+\mu f_Q)}P$. Also, $T_0^{0(D)}$, $T_1^{1(D)}$ and $T_2^{2(D)}$ represent the $f(R,T,Q)$ correction terms and make the field equations more complex. These components are given in Appendix A. Here, prime means $\frac{\partial}{\partial r}$.

The EMT in this theory, unlike GR and $f(R)$, has non-zero divergence due to curvature-matter coupling that contributes to violation of the equivalence principle. Therefore, in the gravitational field, moving particles do not follow geodesic path due to the extra force that acts on these particles. Thus we obtain

$$\nabla^{\rho}T_{\rho\eta} = \frac{2}{2f_T + Rf_Q + 16\pi}\left[\nabla_{\eta}(\mathcal{L}_m f_T) + \nabla_{\rho}(f_Q R^{\pi\rho}T_{\pi\eta}) - G_{\rho\eta}\nabla^{\rho}(f_Q\mathcal{L}_m)\right.$$
$$\left. - \frac{1}{2}(f_T g_{\pi\beta} + f_Q R_{\pi\beta})\nabla_{\eta}T^{\pi\beta}\right]. \tag{11}$$

This leads to the condition of hydrostatic equilibrium as

$$\frac{dP}{dr} + \sigma\frac{d\Theta_1^1}{dr} + \frac{\nu'}{2}(\mu + P) + \frac{\sigma\nu'}{2}\left(\Theta_1^1 - \Theta_0^0\right) + \frac{2\sigma}{r}\left(\Theta_1^1 - \Theta_2^2\right) = \Omega, \tag{12}$$

where the term Ω on right hand side of the above equation appears due to the non-conserved nature of $f(R,T,Q)$ theory whose value is given in Appendix A. Equation (12) may be referred as the generalized form of Tolman-Opphenheimer-Volkoff equation that could help to illustrate systematic changes in the self-gravitating spherically symmetric structure. We obtain a system of four differential Equations (8)–(10) and (12) which involve non-linearity, containing seven unknown parameters $(\nu, \chi, \mu, P, \Theta_0^0, \Theta_1^1, \Theta_2^2)$, thus this system is no more definite. We use systematic method [32] to close the above system and determine the unknowns. For the field Equations (8)–(10), one can define the matter variables as

$$\bar{\mu}^{(eff)} = \mu^{(eff)} - \sigma\Theta_0^0, \quad \bar{P}_r^{(eff)} = P^{(eff)} + \sigma\Theta_1^1, \quad \bar{P}_{\perp}^{(eff)} = P^{(eff)} + \sigma\Theta_2^2. \tag{13}$$

It is obvious from the above terms that anisotropy within self-gravitating system is induced by the source Θ_{η}^{ρ}. This defines the effective parameter of anisotropy as

$$\bar{\Delta}^{(eff)} = \bar{P}_{\perp}^{(eff)} - \bar{P}_{r}^{(eff)} = \sigma\left(\Theta_2^2 - \Theta_1^1\right). \tag{14}$$

It is noticeable here that the component of anisotropy disappears for $\sigma = 0$.

3. Gravitational Decoupling

In this section, we use gravitational decoupling via MGD approach to solve the system (8)–(10). This method serves as a transformation of the field equations such that the newly added factor Θ_{η}^{ρ} supplies the kind of effective equations which may cause the presence of pressure anisotropy in the interior of stellar object. The following metric represents the solution (η, ξ, μ, P) corresponding to the perfect fluid as

$$ds^2 = -e^{\eta}dt^2 + \frac{1}{\xi}dr^2 + r^2d\theta^2 + r^2\sin^2\theta d\vartheta^2, \tag{15}$$

where $\eta = \eta(r)$ and $\xi = \xi(r) = 1 - \frac{2m}{r}$, m is the Misner-Sharp mass of the corresponding object. By imposing the geometrical transformations of linear form on the metric potentials, one can determine the effects of source term Θ_{η}^{ρ} on isotropic models as

$$\eta \to \nu = \eta + \sigma f, \quad \xi \to e^{-\chi} = \xi + \sigma t, \tag{16}$$

where the two geometric deformations t and f are offered to radial and temporal components, respectively. The minimal geometric deformations ($f = 0,\ t \to t^*$) in the above expression guarantees only the effects of additional source in the radial component while the temporal component remains preserved. Consequently, Equation (16) reduces to

$$\eta \to \nu = \eta, \quad \xi \to e^{-\chi} = \xi + \sigma t^*, \tag{17}$$

where $t^* = t^*(r)$. The characteristic feature of this approach is that the source includes the quasi-decoupled system.

To workout the complex system, we divide the field equations into two simple systems. Using the transformations (17) in the system (8)–(10), we obtain the first set corresponding to $\sigma = 0$ as

$$8\pi\left(\mu^{(eff)} - T_0^{0(D)}\right) = e^{-\chi}\left(\frac{\chi'}{r} - \frac{1}{r^2}\right) + \frac{1}{r^2}, \tag{18}$$

$$8\pi\left(P^{(eff)} + T_1^{1(D)}\right) = e^{-\chi}\left(\frac{\nu'}{r} + \frac{1}{r^2}\right) - \frac{1}{r^2}, \tag{19}$$

$$8\pi\left(P^{(eff)} + T_2^{2(D)}\right) = -\frac{e^{-\chi}}{4}\left[\chi'\nu' - \nu'^2 - 2\nu'' + \frac{2\chi'}{r} - \frac{2\nu'}{r}\right], \tag{20}$$

whereas the second set, which contains the source Θ_{η}^{ρ}, becomes

$$8\pi\Theta_0^0 = \frac{t^{*\prime}}{r} + \frac{t^*}{r^2}, \tag{21}$$

$$8\pi\Theta_1^1 = t^*\left(\frac{\nu'}{r} + \frac{1}{r^2}\right), \tag{22}$$

$$8\pi\Theta_2^2 = \frac{t^*}{4}\left[2\nu'' + \nu'^2 - \nu'\chi' + \frac{2\nu'}{r} - \frac{2\chi'}{r}\right]. \tag{23}$$

The system (21)–(23) is analogous to the spherical stellar object having anisotropy with material variables $\bar{\mu}^{(eff)} = \Theta_0^0$, $\bar{P}_r^{(eff)} = -\Theta_1^1$, $\bar{P}_{\perp}^{(eff)} = -\Theta_2^2$ express the geometry

$$ds^2 = -e^{\nu}dt^2 + \frac{1}{t^*}dr^2 + r^2d\theta^2 + r^2\sin^2\theta d\vartheta^2. \tag{24}$$

However, Equations (21)–(23) are not typical field equations for anisotropic spherical source as they differ by a single term $\frac{1}{r^2}$ and thus the matter components become $\bar{\mu}^{(eff)} = \Theta_0^{*0} = \Theta_0^0 + \frac{1}{8\pi r^2}$, $\bar{P}_r^{(eff)} = \Theta_1^{*1} = \Theta_1^1 + \frac{1}{8\pi r^2}$, $\bar{P}_{\perp}^{(eff)} = \Theta_2^{*2} = \Theta_2^2 = \Theta_3^{*3} = \Theta_3^3$. The MGD technique has therefore converted the complex system (8)–(10) into a set of equations describing the isotropic fluid $(\mu^{(eff)}, P^{(eff)}, \nu, \chi)$ along with four unknowns $(t^*, \Theta_0^0, \Theta_1^1, \Theta_2^2)$ obeying the above anisotropic system. As a result, we have decoupled the system (8)–(10) successfully.

The junction conditions are very significant to examine the stellar bodies. One can determine the fundamental characteristics of a star via smooth matching of the exterior and interior regions. In this case, MGD achieves the interior geometry expressed with the help of following metric as

$$ds^2 = -e^{\nu}dt^2 + \frac{1}{\left(1 - \frac{2\tilde{m}(r)}{r}\right)}dr^2 + r^2d\theta^2 + r^2\sin^2\theta d\vartheta^2, \tag{25}$$

where the interior mass is $\tilde{m}(r) = m(r) - \frac{\sigma r}{2}t^*(r)$. To match the inner and outer sectors of a compact star smoothly, we take the general outer metric as

$$ds^2 = -e^{\nu}dt^2 + e^{\chi}dr^2 + r^2d\theta^2 + r^2\sin^2\theta d\vartheta^2. \tag{26}$$

There are two fundamental forms of junction conditions from which the first one ($[ds^2]_{\Sigma} = 0$, where Σ is the hypersurface) yields

$$\nu_-(\mathcal{R}) = \nu_+(\mathcal{R}), \quad e^{-\chi_+(\mathcal{R})} = 1 - \frac{2M_0}{\mathcal{R}} + \sigma t^*(\mathcal{R}), \tag{27}$$

where we have used $\xi = e^{-\chi} - \sigma t^*$. The plus and minus signs represent outer and inner geometries, respectively. Also, $t^*(\mathcal{R})$ and $M_0 = m(\mathcal{R})$ represent the deformation and total mass at the boundary $r = \mathcal{R}$. Further, the second form ($[T_{\rho\eta}w^{\eta}]_{\Sigma} = 0$) gives

$$P^{(eff)}(\mathcal{R}) + \sigma\Big(\Theta_1^1(\mathcal{R})\Big)_- + \Big(T_1^{1(D)}(\mathcal{R})\Big)_- = \sigma\Big(\Theta_1^1(\mathcal{R})\Big)_+ + \Big(T_1^{1(D)}(\mathcal{R})\Big)_+. \tag{28}$$

Using Equation (27), the above equation becomes

$$P^{(eff)}(\mathcal{R}) + \sigma\Big(\Theta_1^1(\mathcal{R})\Big)_- = \sigma\Big(\Theta_1^1(\mathcal{R})\Big)_+, \tag{29}$$

which, in return, gives

$$P^{(eff)}(\mathcal{R}) + \frac{\sigma t^*(\mathcal{R})}{8\pi}\left(\frac{\nu'}{\mathcal{R}} + \frac{1}{\mathcal{R}^2}\right) = \frac{\sigma h^*(\mathcal{R})}{8\pi\mathcal{R}^2}\left(\frac{\mathcal{R}}{\mathcal{R} - 2\mathcal{M}}\right), \tag{30}$$

where $\mathcal{M}$ is mass of the exterior geometry and h^* denotes the exterior geometric deformation in radial component for the Schwarzschild metric in the presence of Θ_{η}^{ρ} (source) given by

$$ds^2 = -\left(1 - \frac{2\mathcal{M}}{r}\right)dt^2 + \frac{1}{\left(1 - \frac{2\mathcal{M}}{r} + \sigma h^*\right)}dr^2 + r^2d\theta^2 + r^2\sin^2\theta d\vartheta^2. \tag{31}$$

The two Equations (27) and (30) provide the appropriate and adequate conditions for discussing the relationship between the MGD inner and outer Schwarzschild spacetimes included by Θ_{η}^{ρ}. One may take the usual Schwarzschild solution, (i.e., $h^* = 0$) as outer geometry, then Equation (30) yields

$$\bar{P}^{(eff)}(\mathcal{R}) \equiv P^{(eff)}(\mathcal{R}) + \frac{\sigma t^*(\mathcal{R})}{8\pi}\left(\frac{1}{\mathcal{R}^2} + \frac{\nu'}{\mathcal{R}}\right) = 0. \tag{32}$$

4. Anisotropic Solutions

We take isotropic spherical solution in modified scenario to solve the field equations corresponding to anisotropic matter configuraton by means of MGD approach. In order to continue our analysis, we take the Krori-Barua solution [45] whose nature is non-singular. This solution was originally developed in GR to discuss the evolution of compact stars, but now we utilize it to construct solutions in modified theory which produce much complicated effective physical quantities. In $f(R,T,Q)$ framework, the solution takes the form

$$e^{\nu} = e^{\mathcal{B}r^2+\mathcal{C}}, \tag{33}$$

$$e^{\chi} = \xi^{-1} = e^{\mathcal{A}r^2}, \tag{34}$$

$$\mu^{(eff)} = -\frac{1}{8\pi r^2}\left[e^{-\mathcal{A}r^2}\left(1-2\mathcal{A}r^2\right)-1\right] + T_0^{0(D)}, \tag{35}$$

$$P^{(eff)} = \frac{1}{8\pi r^2}\left[e^{-\mathcal{A}r^2}\left(1+2\mathcal{B}r^2\right)-1\right] - T_1^{1(D)}, \tag{36}$$

where the unknowns $\mathcal{A}$, $\mathcal{B}$ and $\mathcal{C}$ can be calculated by means of smooth matching. The continuity of g_{tt}, g_{rr} and $g_{tt,r}$ (metric components) between the inner and outer regions takes the form

$$g_{tt} = e^{\mathcal{B}\mathcal{R}^2+C} = 1-\frac{2M_0}{\mathcal{R}}, \tag{37}$$

$$g_{rr} = e^{-\mathcal{A}\mathcal{R}^2} = 1-\frac{2M_0}{\mathcal{R}}, \tag{38}$$

$$\frac{\partial g_{tt}}{\partial r} = \mathcal{B}\mathcal{R}e^{\mathcal{B}\mathcal{R}^2+\mathcal{C}} = \frac{M_0}{\mathcal{R}^2}, \tag{39}$$

which after solving simultaneously leads to

$$\mathcal{A} = \frac{1}{\mathcal{R}^2}\ln\left(\frac{\mathcal{R}}{\mathcal{R}-2M_0}\right), \quad \mathcal{B} = \frac{M_0}{\mathcal{R}^3}\left(1-\frac{2M_0}{\mathcal{R}}\right)^{-1}, \tag{40}$$

$$\mathcal{C} = \ln\left(\frac{\mathcal{R}-2M_0}{\mathcal{R}}\right) - \frac{M_0}{\mathcal{R}}\left(1-\frac{2M_0}{\mathcal{R}}\right)^{-1}, \tag{41}$$

with compactness $\frac{2M_0}{\mathcal{R}} < \frac{8}{9}$. At boundary, these equations guarantee consistency of the solution (33)–(36) (which we have calculated for inner geometry) with the outer region and will be modified undoubtedly after adding the additional source. Equations (17) and (33) provide the radial and temporal metric components that will be used for the construction of anisotropic solution, i.e., for $\sigma \neq 0$ in the inner geometry. The relation between source Θ_η^ρ and geometric deformation t^* has been expressed through Equations (21)–(23). Further, we study a particular compact star, namely $4U1820-30$ with mass $M_0 = 1.58 \pm 0.06 M_\odot$ and radius $\mathcal{R} = 9.1 \pm 0.4$ km [46]. The graphical analysis of all physical attributes is done by using this data.

Next, we make use of some constraints to develop two feasible solutions in the following subsections.

4.1. Solution I

Here, we choose a constraint depending on Θ_1^1 and calculate both t^* as well as Θ_η^ρ to obtain the required solution. Equation (32) points out the compatibility of Schwarzschild exterior geometry with interior spacetime as long as $P^{(eff)}(\mathcal{R}) + T_1^{1(D)}(\mathcal{R}) \sim \sigma\left(\Theta_1^1(\mathcal{R})\right)_-$. The easiest choice is [32]

$$P^{(eff)}+T_1^{1(D)}=\Theta_1^1 \quad \Rightarrow \quad t^*=\xi-\frac{1}{1+\nu' r}, \tag{42}$$

where we have used Equations (19) and (22). Using this equation, we obtain

$$e^{-\chi}=(1+\sigma)\xi-\frac{\sigma}{1+2\mathcal{B}r^2}. \tag{43}$$

The two Equations (33) and (43) contain the metric components which characterize the Krori-Barua solution minimally deformed by Θ_η^ρ. It is necessary to stress that the standard isotropic solutions (33)–(36) can be found by taking $\sigma \to 0$. The continuity of the first fundamental form gives

$$\mathcal{R}e^{\mathcal{B}\mathcal{R}^2+\mathcal{C}}=\mathcal{R}-2\mathcal{M}, \tag{44}$$

and

$$(1+\sigma)\xi-\frac{\sigma}{1+2\mathcal{B}\mathcal{R}^2}=1-\frac{2\mathcal{M}}{\mathcal{R}}. \tag{45}$$

The second fundamental form ($P^{(eff)}(\mathcal{R})+T_1^{1(D)}(\mathcal{R})-\sigma\big(\big(\Theta_1^1(\mathcal{R})\big)\big)_-=0$) together with Equation (42) yields

$$P^{(eff)}(\mathcal{R})+T_1^{1(D)}(\mathcal{R})=0 \quad \Rightarrow \quad \mathcal{A}=\frac{\ln\left(1+2\mathcal{B}\mathcal{R}^2\right)}{\mathcal{R}^2}. \tag{46}$$

Also, Equation (45) leads to the Schwarzschild mass as

$$\frac{2\mathcal{M}}{\mathcal{R}}=\frac{2M_0}{\mathcal{R}}-\sigma\left(1-\frac{2M_0}{\mathcal{R}}\right)+\frac{\sigma}{1+2\mathcal{B}\mathcal{R}^2}. \tag{47}$$

Inserting this in Equation (44), we have

$$e^{\mathcal{B}\mathcal{R}^2+\mathcal{C}}=(1+\sigma)\left(1-\frac{2M_0}{\mathcal{R}}\right)-\frac{\sigma}{1+2\mathcal{B}\mathcal{R}^2}. \tag{48}$$

This equation gives the constant $\mathcal{C}$ in terms of $\mathcal{B}$. The system of Equations (46)–(48) offers necessary and sufficient limitations to do smooth matching between inner and outer spacetimes. Hence, the anisotropic solution for the case (42) is constructed as

$$\begin{aligned}
\bar{\mu}^{(eff)} &= \frac{1}{8\pi r^2}\left[e^{-\mathcal{A}r^2}\left(2\mathcal{A}r^2-1\right)(1+\sigma)+1\right]+\frac{1}{8\pi r^2(1+2\mathcal{B}r^2)^2} \\
&\times \left[\sigma-2\sigma\mathcal{B}r^2+8\pi r^2\left(1+4\mathcal{B}r^2+4\mathcal{B}^2r^4\right)T_0^{0(D)}\right], &(49)\\
\bar{P}_r^{(eff)} &= \frac{1}{8\pi r^2}\left[(1+\sigma)\left\{e^{-\mathcal{A}r^2}\left(2\mathcal{B}r^2+1\right)-1\right\}-8\pi r^2T_1^{1(D)}\right], &(50)\\
\bar{P}_\perp^{(eff)} &= \frac{1}{8\pi r^2}\left[e^{-\mathcal{A}r^2}\left\{1+2\mathcal{B}r^2(1+\sigma)+\sigma\mathcal{B}r^4(\mathcal{B}-\mathcal{A})-\sigma\mathcal{A}r^2\right\}-1\right. \\
&- \left.8\pi r^2T_1^{1(D)}\right]-\frac{\sigma}{8\pi(1+2\mathcal{B}r^2)}\left[\mathcal{B}+(\mathcal{B}-\mathcal{A})\left(1+\mathcal{B}r^2\right)\right], &(51)\\
\bar{\Delta}^{(eff)} &= \frac{\sigma}{8\pi r^2}\left(e^{-\mathcal{A}r^2}-\frac{1}{1+2\mathcal{B}r^2}\right)\left(\mathcal{B}^2r^4-\mathcal{A}\mathcal{B}r^4-\mathcal{A}r^2-1\right). &(52)
\end{aligned}$$

4.2. Solution II

In this case, we take another constraint to obtain second anisotropic solution. The constraint is taken as

$$\mu^{(eff)}-T_0^{0(D)}=\Theta_0^0. \tag{53}$$

Making use of Equations (18) and (21), we have

$$t^{*\prime}+\frac{t^*}{r}-\frac{1}{r}\left[e^{-\mathcal{A}r^2(2\mathcal{A}r^2-1)}+1\right]=0, \tag{54}$$

which gives

$$t^* = \frac{\mathfrak{a}_1}{r} + e^{-\mathcal{A}r^2} - 1, \tag{55}$$

where $\mathfrak{a}_1$ is the constant of integration. The nature of a solution at the core of star should be non-singular, thus we take $\mathfrak{a}_1 = 0$ giving

$$t^* = e^{-\mathcal{A}r^2} - 1. \tag{56}$$

One can achieve the matching conditions by implementing the same approach as for the first solution given as

$$2(\mathcal{M} - M_0) + \sigma\mathcal{R}\left(e^{-\mathcal{A}r^2} - 1\right) = 0, \tag{57}$$

$$\mathcal{B}\mathcal{R}^2 + \mathcal{C} = \ln\left[1 - \frac{2M_0}{\mathcal{R}} + \sigma\mathcal{R}\left(e^{-\mathcal{A}r^2} - 1\right)\right]. \tag{58}$$

Finally, the expressions of $\bar{\mu}^{(eff)}$, $\bar{P}_r^{(eff)}$, $\bar{P}_\perp^{(eff)}$ and $\bar{\Delta}^{(eff)}$ are

$$\bar{\mu}^{(eff)} = \frac{1}{8\pi r^2}\left[(1+\sigma)\left\{e^{-\mathcal{A}r^2}\left(2\mathcal{A}r^2 - 1\right) + 1\right\} + 8\pi r^2 T_0^{0(D)}\right], \tag{59}$$

$$\bar{P}_r^{(eff)} = \frac{1}{8\pi r^2}\left[(1+\sigma)\left\{e^{-\mathcal{A}r^2}\left(2\mathcal{B}r^2 + 1\right) - 1\right\} - 2\sigma\mathcal{B}r^2 - 8\pi r^2 T_1^{1(D)}\right], \tag{60}$$

$$\begin{aligned}\bar{P}_\perp^{(eff)} = \frac{1}{8\pi r^2}\Big[&e^{-\mathcal{A}r^2}\left\{1 + 2\mathcal{B}r^2(1+\sigma) + \sigma\left(\mathcal{B}^2r^4 - \mathcal{A}\mathcal{B}r^4 - \mathcal{A}r^2\right)\right\} - 1 \\ &- \sigma r^2\left(2\mathcal{B} + \mathcal{B}^2r^2 - \mathcal{A}\mathcal{B}r^2 - \mathcal{A}\right) - 8\pi r^2 T_1^{1(D)}\Big],\end{aligned} \tag{61}$$

$$\bar{\Delta}^{(eff)} = \frac{\sigma}{8\pi r^2}\left[r^2\left(e^{-\mathcal{A}r^2} - 1\right)\left(\mathcal{B}^2r^2 - \mathcal{A}\mathcal{B}r^2 - \mathcal{A}\right) - e^{-\mathcal{A}r^2} - 4\mathcal{B}r^2 + 1\right]. \tag{62}$$

4.3. Physical Interpretation of the Obtained Solutions

The mass of a sphere can be determined as

$$m(r) = 4\pi\int_0^{\mathcal{R}} r^2\bar{\mu}^{(eff)}dr. \tag{63}$$

where the quantity $\bar{\mu}^{(eff)}$ describes the energy density in $f(R,T,Q)$ gravity, whose value is provided in Equations (49) and (59) in case of the solutions I and II, respectively. The mass of anisotropic star can be obtained by solving this equation numerically with condition at the center as $m(0) = 0$. The compactness factor $(\zeta(r))$ is another significant feature of self-gravitating system. It is defined as the ratio of mass and radius of a stellar structure. Buchdahl [47] found the maximum value of $\zeta(r)$ by matching the inner static spherical spacetime with outer Schwarzschild solution. For a stable star, this limit is defined as $\zeta(r) = \frac{m}{\mathcal{R}} < \frac{4}{9}$, where $m(r) = \frac{\mathcal{R}}{2}(1 - e^{-\chi})$. The redshift $(D(r))$ of a self-gravitating body measures the increment in wavelength of electromagnetic diffusion because of the gravitational pull practiced by that body, which is given as $D(r) = \frac{1}{\sqrt{1-2\zeta}} - 1$. Buchdahl confined its value at the surface of star as $D(r) < 2$ for a perfect matter distribution. However, its upper bound becomes 5.211 for anisotropic configured stellar bodies [48].

The energy conditions are used to check the existence of ordinary matter in the interior and viability of the resulting solutions. These constraints are followed by the parameters governing the inner region of the stellar objects which are made of ordinary matter. We can categorize these bounds into dominant, strong, weak and null energy conditions. The energy conditions in $f(R,T,Q)$ theory turn out to be

$$\begin{aligned}&\bar{\mu}^{(eff)} \geq 0, \quad \bar{\mu}^{(eff)} + \bar{P}_r^{(eff)} \geq 0, \\ &\bar{\mu}^{(eff)} + \bar{P}_\perp^{(eff)} \geq 0, \quad \bar{\mu}^{(eff)} - \bar{P}_r^{(eff)} \geq 0,\end{aligned}$$

$$\bar{\mu}^{(eff)} - \bar{P}_{\perp}^{(eff)} \geq 0, \quad \bar{\mu}^{(eff)} + \bar{P}_{r}^{(eff)} + 2\bar{P}_{\perp}^{(eff)} \geq 0. \tag{64}$$

The stability of a stellar object is found to be a key factor in astrophysics to analyze a feasible system. We examine stability by taking the causality condition according to which the square of sound speed within the geometrical structure must lie in the range $[0, 1]$, i.e., $0 \leq v_s^2 < 1$. For anisotropic matter configuration, the difference between sound speeds in tangential ($v_{s\perp}^2 = \frac{dP_\perp}{d\mu}$) and radial directions ($v_{sr}^2 = \frac{dP_r}{d\mu}$) can be used to check the stable region of compact structures as $\mid v_{s\perp}^2 - v_{sr}^2 \mid < 1$ [49]. The term $v_s^2 = v_{sr}^2 + v_{s\perp}^2$ also guarantees stability of the resulting solution if it is less than one throughout the structure. An adiabatic index (Γ) also plays a crucial role in analyzing the stability of compact stars. For a stable stellar structure, the value of Γ should not be less than $\frac{4}{3}$ [50–52]. Here, $\Gamma^{(eff)}$ can be expressed as

$$\Gamma^{(eff)} = \frac{\bar{\mu}^{(eff)} + \bar{P}_r^{(eff)}}{\bar{P}_r^{(eff)}} \left(\frac{d\bar{P}_r^{(eff)}}{d\bar{\mu}^{(eff)}} \right). \tag{65}$$

In order to discuss physical viability and stability of the obtained solutions, we take the following model [15]

$$f(R, T, R_{\rho\eta} T^{\rho\eta}) = R + \alpha R_{\rho\eta} T^{\rho\eta}, \tag{66}$$

where α works as the coupling constant. Here, α can be positive or negative. For its positive values, the matter variables such as energy density and radial/tangential pressures corresponding to both resulting solutions do not show acceptable behavior. Thus, we are left only with negative values of α and we take it as -0.3 to analyze physical nature of the solution I and fix the constant $\mathcal{A}$ calculated in Equation (46). The remaining two constants $\mathcal{B}$ and $\mathcal{C}$ are given in Equations (40) and (41). Figure 1 (left) shows mass of the geometry (6) for $\sigma = 0.1$ and 0.9. It is observed that mass increases with rise in the decoupling parameter σ. The other two plots of Figure 1 point out that the ranges of compactness factor and redshift parameter agree with their respective bounds.

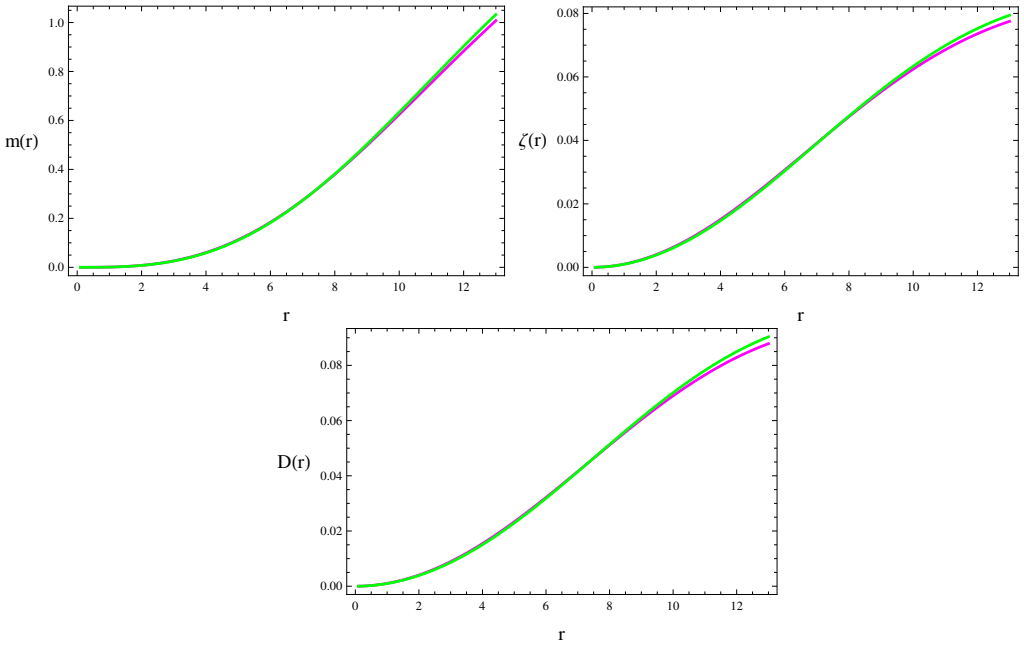

Figure 1. Graphical analysis of mass, compactness and redshift parameters corresponding to $\sigma = 0.1$ (pink) and $\sigma = 0.9$ (green) for solution I.

For an astrophysical object, the value of material variables (such as energy density and radial as well as tangential pressures) should be finite, maximum and positive at the center. Further, their behavior towards the star's boundary must be monotonically decreasing.

One can analyze from Figure 2 (upper left) that the energy density involving $f(R,T,Q)$ corrections is maximal at the center while shows linearly decreasing behavior towards boundary. It is noted that the increment in σ also decreases energy density. The graphical nature of $\bar{P}_r^{(eff)}$ and $\bar{P}_\perp^{(eff)}$ is shown similar to each other for the parameter α. By increasing the value of r, both ingredients decrease as well as there is a gradual linear increment in $\bar{P}_\perp^{(eff)}$ with rise in σ as compared to $\bar{P}_r^{(eff)}$. The factor $\bar{\Delta}^{(eff)}$ in Figure 2 (lower right) shows positive behavior and increases with the increase in the decoupling parameter σ. This indicates that σ generates stronger anisotropy in the structure. The values of radial and tangential pressures are equal at the center thus anisotropy disappears at that point. The system will be considered viable if it meets all the energy bounds (64). Figure 3 shows that our developed anisotropic solution I is physically viable as all energy conditions are satisfied. Figure 4 demonstrates that the solution I (49)–(52) fulfills stability criteria for all values of the decoupling parameter.

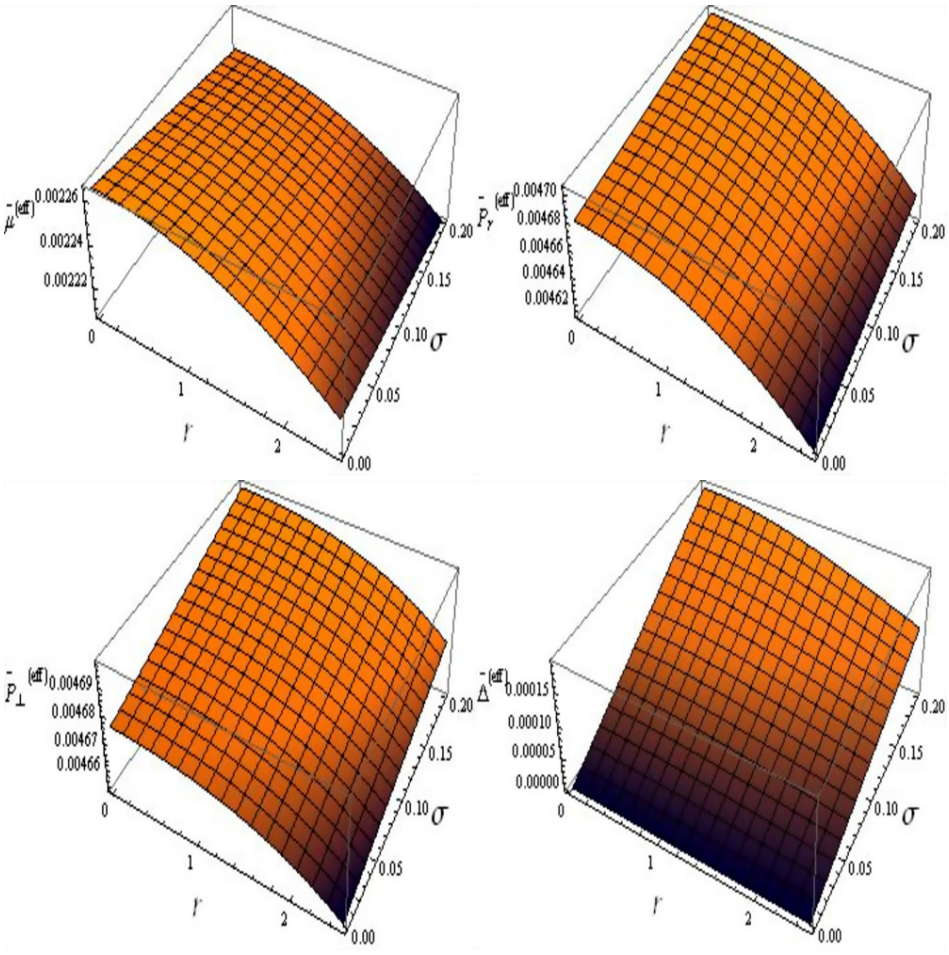

Figure 2. Graphical analysis of $\bar{\mu}^{(eff)}$, $\bar{P}_r^{(eff)}$, $\bar{P}_\perp^{(eff)}$ and $\bar{\Delta}^{(eff)}$ versus r and σ for solution I.

Now we explore physical features of the second solution by taking same value of α as for solution I. The constants $\mathcal{A}$ and $\mathcal{B}$ are presented in Equations (40) and (58). Figure 5 (upper left) indicates that the mass of self-gravitating body shows decreasing behavior as the parameter σ increases. The parameters $D(r)$ and $\zeta(r)$ also meet the desired limits as can be seen from Figure 5. The physical behavior of $\bar{\mu}^{(eff)}$, $\bar{P}_r^{(eff)}$, $\bar{P}_\perp^{(eff)}$ and $\bar{\Delta}^{(eff)}$ is shown in Figure 6. When one increases the value of σ, $\bar{\mu}^{(eff)}$ and both effective pressure components show increasing and decreasing behavior, respectively. The lower right plot in Figure 6 indicates that $\bar{\Delta}^{(eff)}$ shows increasing behavior with the rise in σ which produces stronger anisotropy in the system. Figure 7 guarantees the regular behavior

of both solutions as $\frac{d\bar{\mu}^{(eff)}}{dr} < 0$, $\frac{d\bar{P}_r^{(eff)}}{dr} < 0$ and $\frac{\bar{P}_\perp^{(eff)}}{dr} < 0$ everywhere. Figure 8 shows that all energy constraints (64) for solution II are satisfied and hence it is physically viable. Figure 9 reveals that our second solution (59)–(62) is also stable everywhere. Figure 10 also confirms stability of both the developed solutions.

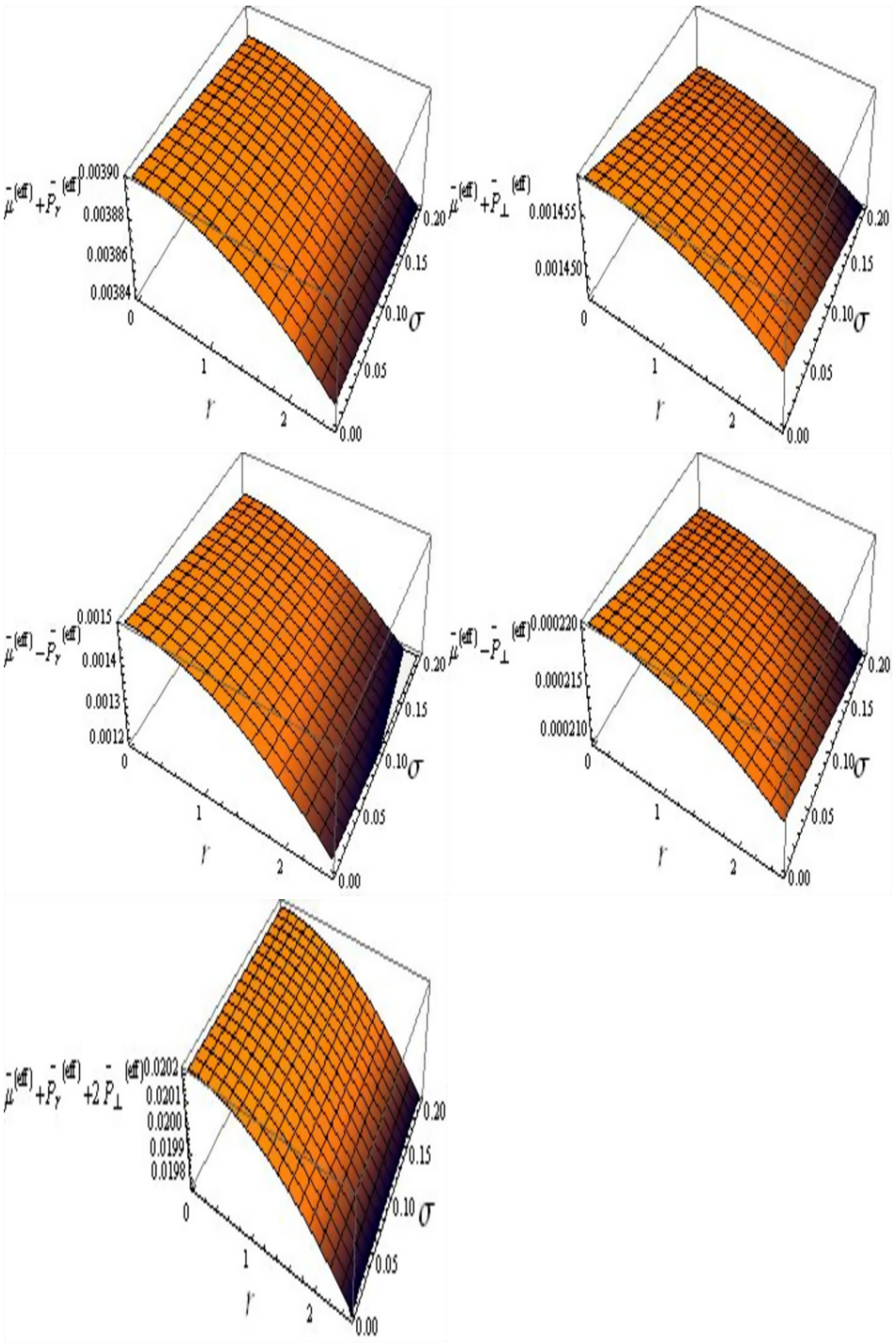

Figure 3. Graphical analysis of energy bounds versus r and σ for solution I.

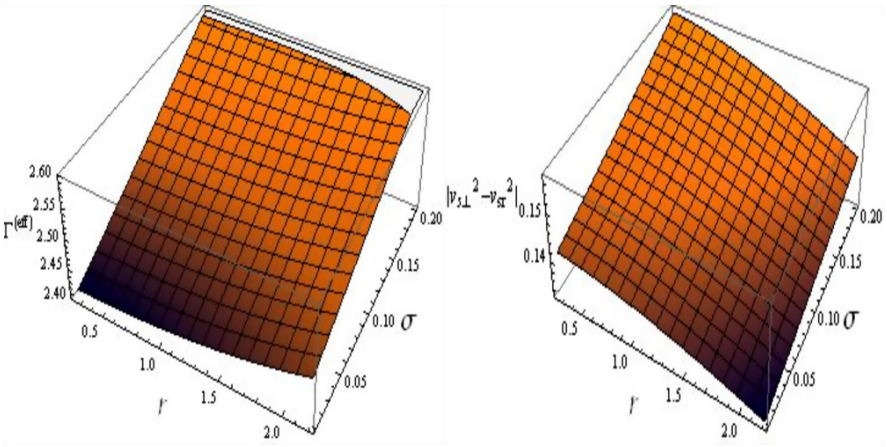

Figure 4. Graphical analysis of adiabatic index and $|v_{s\perp}^2 - v_{sr}^2|$ versus r and σ for solution I.

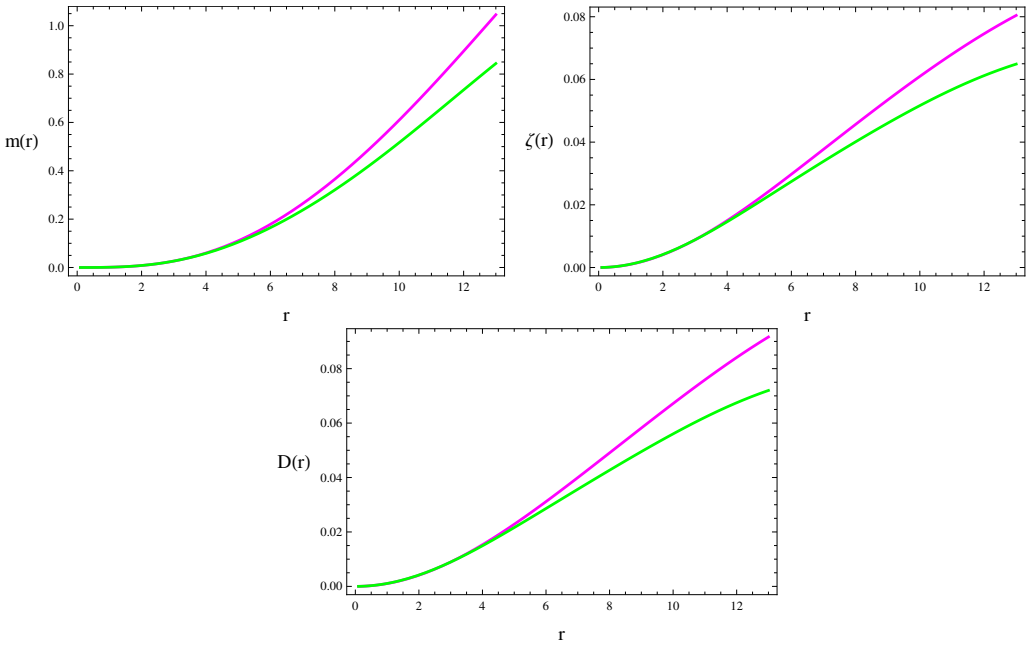

Figure 5. Graphical analysis of mass, compactness and redshift parameters corresponding to $\sigma = 0.1$ (pink) and $\sigma = 0.3$ (green) for solution II.

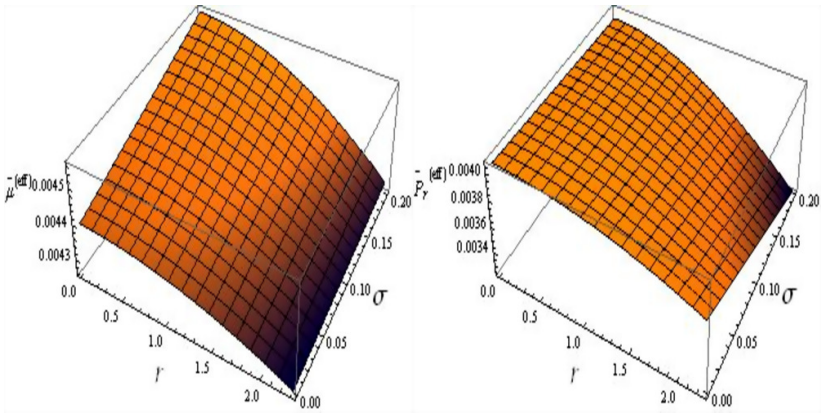

Figure 6. *Cont.*

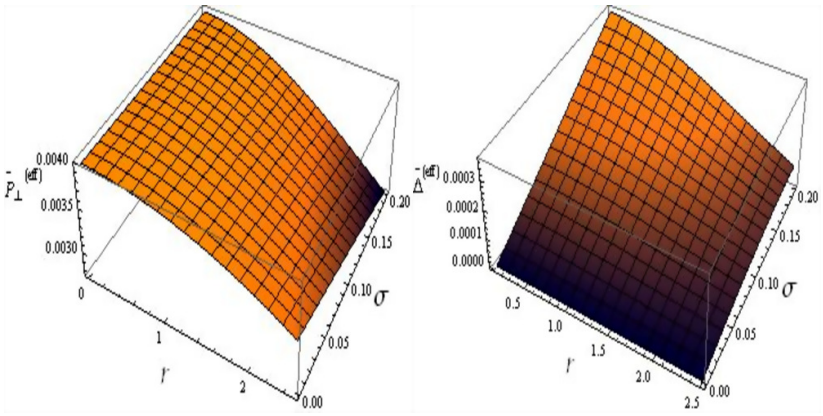

Figure 6. Graphical analysis of $\bar{\mu}^{(eff)}$, $\bar{P}_r^{(eff)}$, $\bar{P}_{\perp}^{(eff)}$ and $\bar{\Delta}^{(eff)}$ versus r and σ for solution II.

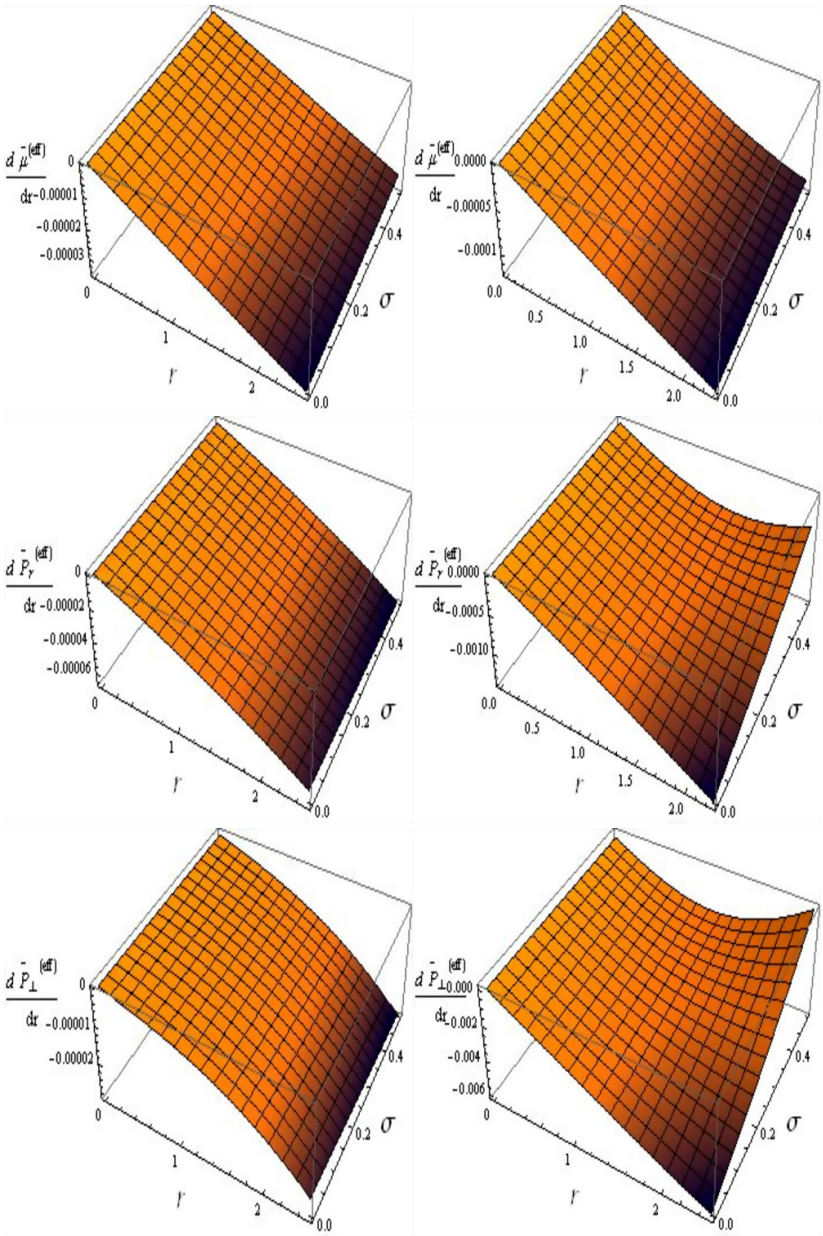

Figure 7. Graphical analysis of $\frac{d\bar{\mu}^{(eff)}}{dr}$, $\frac{d\bar{P}_r^{(eff)}}{dr}$ and $\frac{\bar{P}_{\perp}^{(eff)}}{dr}$ versus r and σ corresponding to solution I (**left**) and solution II (**right**).

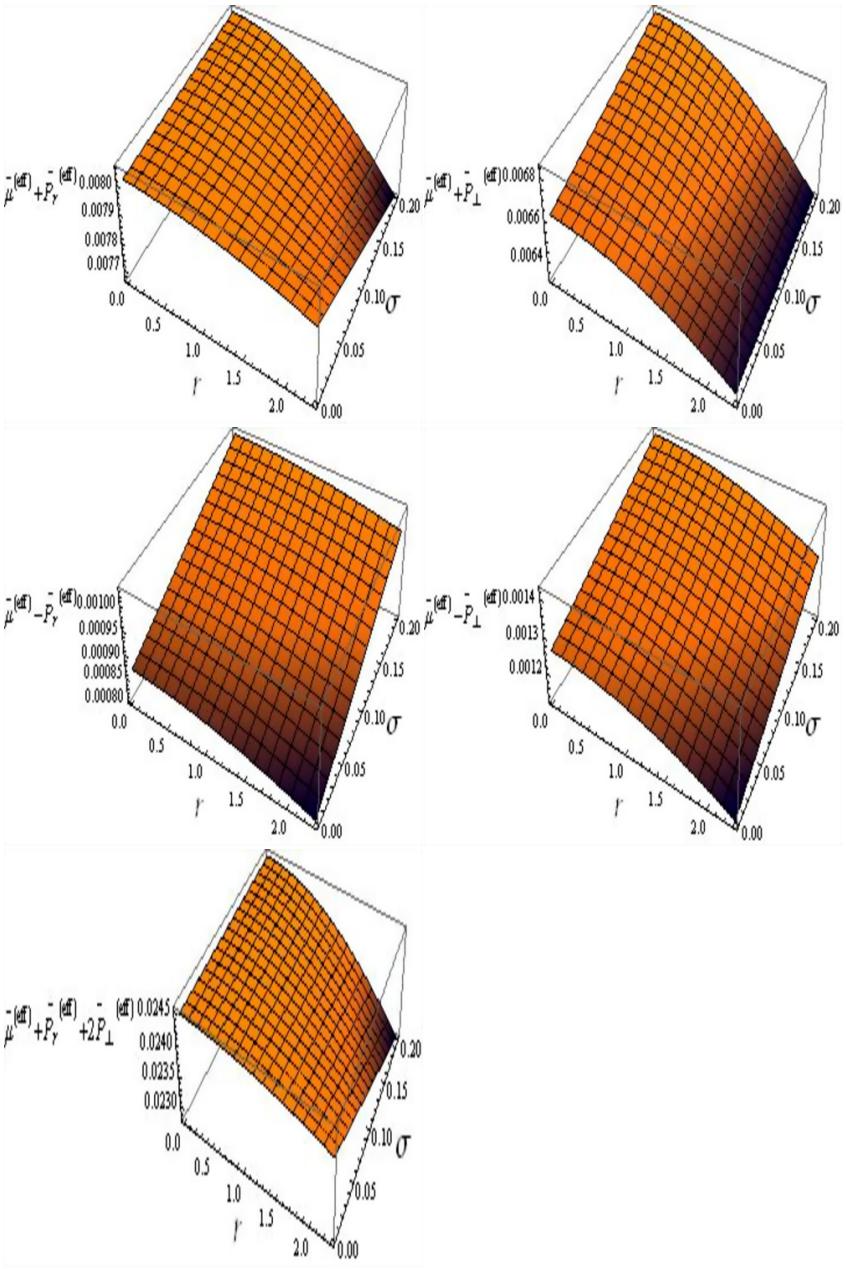

Figure 8. Graphical analysis of energy bounds versus r and σ for solution II.

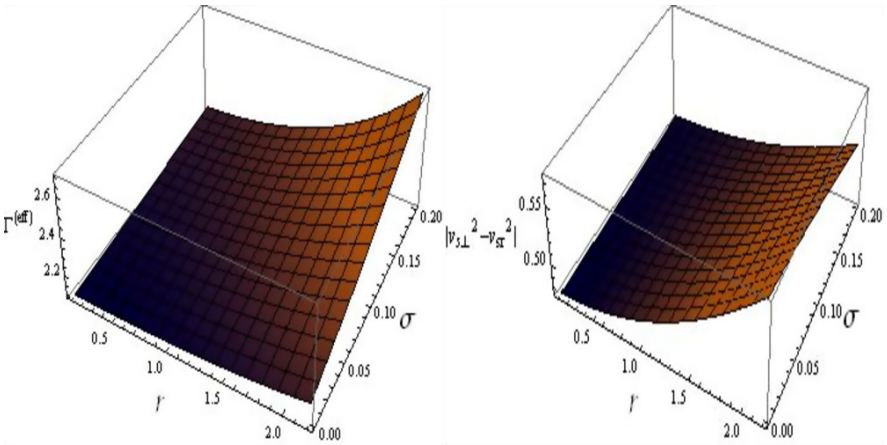

Figure 9. Graphical analysis of adiabatic index and $|v_{s\perp}^2 - v_{sr}^2|$ versus r and σ for solution II.

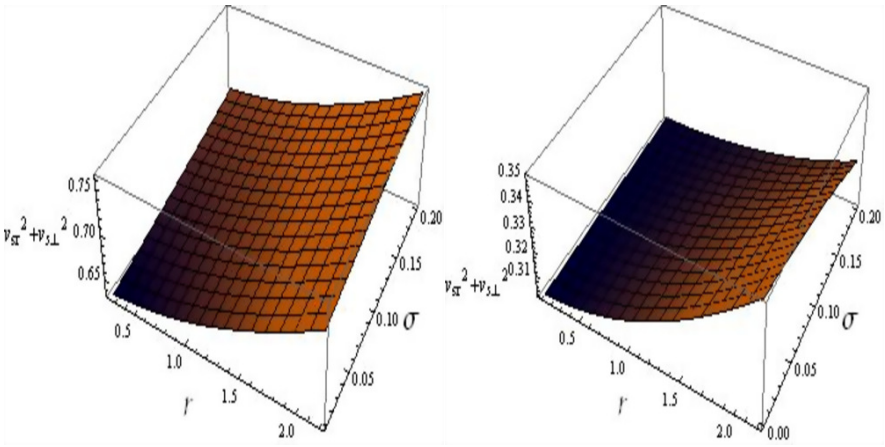

Figure 10. Graphical analysis of $v_{sr}^2 + v_{s\perp}^2$ versus r and σ for solution I (**left**) and solution II (**right**).

5. Conclusions

This paper is devoted to studying anisotropic spherical solutions of self-gravitating object through gravitational decoupling technique in $f(R, T, Q)$ theory. Here, we have used a linear model $R + \alpha Q$ of this curvature-matter coupled gravity. Two anisotropic solutions have been obtained by adding an extra term $\Theta_{\rho\eta}$ in the isotropic solution. We have taken the Krori-Barua ansatz and determined unknown quantities by means of matching criteria. There are four unknown quantities in the second sector (21)–(23) which are reduced by implementing an extra constraint on $\Theta_{\rho\eta}$.

We have utilized two constraints which equal the effective pressure and energy density of the original isotropic distribution and additional anisotropic source to develop solutions I and II, respectively. The physical behavior of state variables $(\bar{\mu}^{(eff)}, \bar{P}_r^{(eff)}, \bar{P}_\perp^{(eff)})$, anisotropy $(\bar{\Delta}^{(eff)})$ and energy conditions (64) are examined for $\alpha = -0.3$ to assess the acceptance of these solutions. It is found that our both solutions fulfil the needed limit for compactness and redshift. It is obtained that stellar structure corresponding to the solution I becomes more dense for larger values of the decoupling parameter σ, whereas it becomes less dense for the solution II. The stability of the resulting solutions has also been examined through cracking approach and the adiabatic index. We have found that both solutions meet the stability criteria and also physically viable as they fulfil the energy bounds. It is worth mentioning here that our resulting solutions are physically viable as well as stable for larger values of σ contrary to GR and $f(G)$ gravity [33,34]. Thus, this technique in $f(R, T, Q)$ gravity provides more suitable results. Our results are consistent with $f(R)$ theory [36]. Finally, we would like to mention here that all these findings reduce to GR when $\alpha = 0$ in the model (66).

Author Contributions: M.S. suggested the research problem and finalized the manuscript while T.N. did the calculations and prepared the initial draft. All authors have read and agreed to the published version of the manuscript.

Funding: This research received no external funding.

Institutional Review Board Statement: Not applicable.

Informed Consent Statement: Not applicable.

Data Availability Statement: No data was used.

Conflicts of Interest: There is no conflict of interest.

Appendix A

The matter components involving modified corrections appearing in Equations (8)–(10) are

$$
\begin{aligned}
T_0^{0(D)} &= \frac{1}{8\pi(f_R+\mu f_Q)}\Bigg[\mu\Bigg\{f_Q\left(\frac{\nu'\chi'}{4e^{\chi}}-\frac{\nu'}{re^{\chi}}+\frac{\nu'^2}{2e^{\chi}}-\frac{\nu''}{2e^{\chi}}-\frac{1}{2}R\right)+f'_Q\left(\frac{\nu'}{2e^{\chi}}\right.\\
&+ \left.\frac{1}{re^{\chi}}-\frac{\chi'}{4e^{\chi}}\right)+\frac{f''_Q}{2e^{\chi}}-2f_T\Bigg\}+\mu'\left\{f_Q\left(\frac{\nu'}{2e^{\chi}}-\frac{\chi'}{4e^{\chi}}+\frac{1}{re^{\chi}}\right)+\frac{f'_Q}{e^{\chi}}\right\}\\
&+ \frac{f_Q\mu''}{2e^{\chi}}+P\left\{f_Q\left(\frac{3\chi'^2}{4e^{\chi}}-\frac{\chi''}{2e^{\chi}}-\frac{2}{r^2e^{\chi}}\right)-f'_Q\left(\frac{5\chi'}{4e^{\chi}}-\frac{1}{re^{\chi}}\right)+\frac{f''_Q}{2e^{\chi}}\right\}\\
&+ P'\left\{f_Q\left(\frac{1}{re^{\chi}}-\frac{5\chi'}{4e^{\chi}}\right)+\frac{f'_Q}{e^{\chi}}\right\}+\frac{f_QP''}{2e^{\chi}}+\frac{Rf_R}{2}+f'_R\left(\frac{\chi'}{2e^{\chi}}-\frac{2}{re^{\chi}}\right)\\
&- \frac{f''_R}{e^{\chi}}-\frac{f}{2}\Bigg],\\
T_1^{1(D)} &= \frac{1}{8\pi(f_R+\mu f_Q)}\Bigg[\mu\left(f_T-\frac{f_Q\nu'^2}{4e^{\chi}}+\frac{f'_Q\nu'}{4e^{\chi}}\right)+\frac{f_Q\mu'\nu'}{4e^{\chi}}+P\Bigg\{f_T+f_Q\left(\frac{\nu''}{e^{\chi}}\right.\\
&+ \left.\frac{\nu'^2}{2e^{\chi}}-\frac{\chi'^2}{e^{\chi}}-\frac{3\chi'}{re^{\chi}}-\frac{3\nu'\chi'}{4e^{\chi}}+\frac{2}{r^2e^{\chi}}+\frac{1}{2}R\right)-f'_Q\left(\frac{\nu'}{4e^{\chi}}+\frac{2}{re^{\chi}}\right)\Bigg\}\\
&- P'f_Q\left(\frac{\nu'}{4e^{\chi}}+\frac{2}{re^{\chi}}\right)+\frac{f}{2}-\frac{Rf_R}{2}-f'_R\left(\frac{\nu'}{2e^{\chi}}+\frac{2}{re^{\chi}}\right)\Bigg],\\
T_2^{2(D)} &= \frac{1}{8\pi(f_R+\mu f_Q)}\Bigg[\mu\left(f_T-\frac{f_Q\nu'^2}{4e^{\chi}}+\frac{f'_Q\nu'}{4e^{\chi}}\right)+\frac{f_Q\mu'\nu'}{4e^{\chi}}+P\Bigg\{f_T+f_Q\left(\frac{\chi''}{2e^{\chi}}\right.\\
&- \left.\frac{3\chi'^2}{4e^{\chi}}+\frac{\nu'}{2re^{\chi}}-\frac{\chi'}{2re^{\chi}}-\frac{2}{r^2}+\frac{1}{r^2e^{\chi}}+\frac{1}{2}R\right)+f'_Q\left(\frac{3\chi'}{2e^{\chi}}-\frac{3}{re^{\chi}}-\frac{\nu'}{4e^{\chi}}\right)\\
&- \frac{f''_Q}{e^{\chi}}\Bigg\}+P'\left\{f_Q\left(\frac{3\chi'}{2e^{\chi}}-\frac{3}{re^{\chi}}-\frac{\nu'}{4e^{\chi}}\right)-\frac{2f'_Q}{e^{\chi}}\right\}-\frac{f_QP''}{e^{\chi}}-\frac{Rf_R}{2}+\frac{f}{2}\\
&+ f'_R\left(\frac{\chi'}{2e^{\chi}}-\frac{\nu'}{2e^{\chi}}-\frac{1}{re^{\chi}}\right)-\frac{f''_R}{e^{\chi}}\Bigg].
\end{aligned}
$$

The quantity Ω in Equation (12) is given as

$$
\begin{aligned}
\Omega = \frac{2}{(Rf_Q+2(8\pi+f_T))}&\Bigg[f'_Qe^{-\chi}P\left(\frac{1}{r^2}-\frac{e^{\chi}}{r^2}+\frac{\nu'}{r}\right)+f_Qe^{-\chi}P\left(\frac{\nu''}{r}-\frac{\nu'}{r^2}-\frac{\chi'}{r^2}\right.\\
&- \left.\frac{\nu'\chi'}{r}-\frac{2}{r^3}+\frac{2e^{\chi}}{r^3}\right)+P'\left\{f_Qe^{-\chi}\left(\frac{\nu'\chi'}{8}-\frac{\nu''}{8}-\frac{\nu'^2}{8}+\frac{\chi'}{2r}+\frac{\nu'}{2r}+\frac{1}{r^2}-\frac{e^{\chi}}{r^2}\right)\right.\\
&+ \left.\frac{3}{4}f_T\right\}+Pf'_T-\mu f'_T-\mu'\left\{\frac{3f_T}{2}+\frac{f_Qe^{-\chi}}{8}\left(\nu'^2-\nu'\chi'+2\nu''+\frac{4\nu'}{r}\right)\right\}\\
&+ \left(\frac{1}{r^2}-\frac{e^{-\chi}}{r^2}-\frac{\nu'e^{-\chi}}{r}\right)\left(\mu'f_Q+\mu f'_Q\right)\Bigg].
\end{aligned}
$$

The adiabatic index corresponding to solutions I and II are

$$
\begin{aligned}
\Gamma^{(eff)} = -&\Bigg[\left(2\mathcal{B}r^2\left(\pi\alpha\left(3\mathcal{A}r^2-7\right)-\sigma-1\right)+4\pi\alpha\mathcal{A}r^2+(\sigma+1)e^{\mathcal{A}r^2}+2\pi\alpha\mathcal{B}^2r^4\right.\\
&\left.-\sigma-1\right)\left(e^{\mathcal{A}r^2}\left(8\mathcal{B}^3r^6+4\mathcal{B}^2r^4(3-2\sigma)+6\mathcal{B}r^2(\sigma+1)+\sigma+1\right)-\left(2\mathcal{B}r^2\right.\right.\\
&\left.\left.+1\right)^3\left(-12\pi\alpha\mathcal{A}^3r^6+2\mathcal{A}^2r^4\left(3\pi\alpha\left(\mathcal{B}r^2+2\right)-\sigma-1\right)+\mathcal{A}r^2\left(18\pi\alpha\mathcal{B}^2r^4\right.\right.\right.\\
&\left.\left.\left.-28\pi\alpha\mathcal{B}r^2+\sigma+1\right)-18\pi\alpha\mathcal{B}^2r^4+\sigma+1\right)\right)\Bigg]^{-1}\Bigg[2r^2\left(2\mathcal{B}r^2+1\right)\left(2\pi\alpha\mathcal{A}^2r^4\right.
\end{aligned}
$$

$$\times \left(3\mathcal{B}r^2+2\right)+\mathcal{A}r^2\left(2\pi\alpha\mathcal{B}^2r^4-2\mathcal{B}r^2(10\pi\alpha+\sigma+1)-\sigma-1\right)+(\sigma+1)$$
$$\times e^{\mathcal{A}r^2}-2\pi\alpha\mathcal{B}^2r^4-\sigma-1\big)\big(-6\pi\alpha\mathcal{A}^2\left(2\mathcal{B}r^3+r\right)^2+\mathcal{B}\big(-18\pi\alpha-2\mathcal{B}r^2$$
$$\times \left(31\pi\alpha-\sigma e^{\mathcal{A}r^2}+2\sigma+2\right)+3\sigma e^{\mathcal{A}r^2}+40\pi\alpha\mathcal{B}^3r^6-4\mathcal{B}^2r^4(8\pi\alpha+\sigma+1)$$
$$-\sigma-1)+\mathcal{A}\left(2\mathcal{B}r^2+1\right)^2\left(2\pi\left(\alpha+3\alpha\mathcal{B}r^2\right)-\sigma-1\right)\big)\Big],$$

$$\Gamma^{(eff)}=\Big[\big(12\pi\alpha\mathcal{A}^3r^6+2\mathcal{A}^2r^4\big(-3\pi\alpha\left(\mathcal{B}r^2+2\right)+\sigma+1\big)-\mathcal{A}r^2\big(18\pi\alpha\mathcal{B}^2r^4$$
$$-28\pi\alpha\mathcal{B}r^2+\sigma+1\big)+(\sigma+1)e^{\mathcal{A}r^2}+18\pi\alpha\mathcal{B}^2r^4-\sigma-1\big)\big(2\mathcal{B}r^2\left(\pi\alpha\right.$$
$$\times\left(3\mathcal{A}r^2-7\right)-\sigma-1\big)+e^{\mathcal{A}r^2}\left(2\mathcal{B}r^2\sigma+\sigma+1\right)+4\pi\alpha\mathcal{A}r^2+2\pi\alpha\mathcal{B}^2r^4$$
$$-\sigma-1)\Big]^{-1}\Big[2r^2\big(6\pi\alpha\mathcal{A}^2r^2+\mathcal{A}\big(-2\pi\left(\alpha+3\alpha\mathcal{B}r^2\right)+\sigma+1\big)+\mathcal{B}\big(-\sigma$$
$$\times e^{\mathcal{A}r^2}-2\pi\alpha\left(5\mathcal{B}r^2-9\right)+\sigma+1\big)\big)\left(2\pi\alpha\mathcal{A}^2r^4\left(3\mathcal{B}r^2+2\right)+\mathcal{A}r^2\left(2\pi\alpha\mathcal{B}^2r^4\right.\right.$$
$$\left.\left.-2\mathcal{B}r^2(10\pi\alpha+\sigma+1)-\sigma-1\right)+(\sigma+1)e^{\mathcal{A}r^2}-2\pi\alpha\mathcal{B}^2r^4-\sigma-1\right)\Big].$$

The value of $|v_{st}^2-v_{sr}^2|$ corresponding to solutions I and II become

$$|v_{st}^2-v_{sr}^2|=\Big|\Big[\left(2\mathcal{B}r^2+1\right)^3\big(-12\pi\alpha\mathcal{A}^3r^6+2\mathcal{A}^2r^4\left(3\pi\alpha\left(\mathcal{B}r^2+2\right)-\sigma-1\right)$$
$$+\mathcal{A}r^2\left(18\pi\alpha\mathcal{B}^2r^4-28\pi\alpha\mathcal{B}r^2+\sigma+1\right)-18\pi\alpha\mathcal{B}^2r^4+\sigma+1\big)-e^{\mathcal{A}r^2}$$
$$\times\left(8\mathcal{B}^3r^6+4\mathcal{B}^2r^4(3-2\sigma)+6\mathcal{B}r^2(\sigma+1)+\sigma+1\right)\Big]^{-1}\Big[\left(2\mathcal{B}r^2+1\right)$$
$$\times\big(-\mathcal{B}^2r^4\big(-16\pi\alpha+(16\pi\alpha-4\sigma+3)e^{\mathcal{A}r^2}+5\sigma\big)+\mathcal{A}r^2\left(4\pi\alpha+\mathcal{B}r^2\right.$$
$$\times\left(16\pi\alpha+e^{\mathcal{A}r^2}-3\sigma\right)+4\mathcal{B}^4r^8\sigma+8\mathcal{B}^3r^6\sigma+\mathcal{B}^2r^4(16\pi\alpha+\sigma)-\sigma)$$
$$-4\mathcal{B}r^2(4\pi\alpha-\sigma)\left(e^{\mathcal{A}r^2}-1\right)-r^4\sigma\left(\mathcal{B}r^2+1\right)\left(2\mathcal{A}\mathcal{B}r^2+\mathcal{A}\right)^2+(4\pi\alpha$$
$$-\sigma)\left(1-e^{\mathcal{A}r^2}\right)-4\mathcal{B}^4r^8\sigma-4\mathcal{B}^3r^6\sigma)\Big]\Big|,$$

$$|v_{st}^2-v_{sr}^2|=\Big|\Big[12\pi\alpha\mathcal{A}^3r^6+2\mathcal{A}^2r^4\big(-3\pi\alpha\left(\mathcal{B}r^2+2\right)+\sigma+1\big)-\mathcal{A}r^2\big(18\pi\alpha\mathcal{B}^2r^4$$
$$-28\pi\alpha\mathcal{B}r^2+\sigma+1\big)+(\sigma+1)e^{\mathcal{A}r^2}+18\pi\alpha\mathcal{B}^2r^4-\sigma-1\Big]^{-1}\Big[\sigma\big(\mathcal{A}^2\left(\mathcal{B}r^6\right.$$
$$\left.+r^4\right)+e^{\mathcal{A}r^2}\left(\mathcal{A}\mathcal{B}r^4-\mathcal{B}^2r^4-1\right)+\mathcal{A}\left(-\mathcal{B}^2r^6-\mathcal{B}r^4+r^2\right)+\mathcal{B}^2r^4+1\big)$$
$$+4\pi\alpha\left(-\mathcal{A}r^2+e^{\mathcal{A}r^2}-1\right)\Big]\Big|.$$

References

1. Persic, M.; Salucci, P.; Stel, F. The universal rotation curve of spiral galaxies—I. The dark matter connection. *Mon. Not. R. Astron. Soc.* **1996**, *281*, 27. [CrossRef]
2. Borriello, A.; Salucci, P. The dark matter distribution in disc galaxies. *Mon. Not. R. Astron. Soc.* **2001**, *323*, 285. [CrossRef]
3. Nojiri, S.; Odintsov, S.D. Modified gravity with negative and positive powers of curvature: Unification of inflation and cosmic acceleration. *Phys. Rev. D* **2003**, *68*, 123512. [CrossRef]
4. Cognola, G.; Elizalde, E.; Nojiri, S.I.; Odintsov, S.D.; Zerbini, S. One-loop $f(R)$ gravity in de Sitter universe. *J. Cosmol. Astropart. Phys.* **2005**, *2005*, 010. [CrossRef]
5. Song, Y.-S.; Hu, W.; Sawicki, I. Large scale structure of $f(R)$ gravity. *Phys. Rev. D* **2007**, *75*, 044004. [CrossRef]
6. Capozziello, S.; De Laurentis, M.; Odintsov, S.D.; Stabile, A. Hydrostatic equilibrium and stellar structure in $f(R)$ gravity. *Phys. Rev. D* **2011**, *83*, 064004. [CrossRef]

7. Sharif, M.; Kausar, H.R. Effects of $f(R)$ model on the dynamical instability of expansionfree gravitational collapse. *J. Cosmol. Astropart. Phys.* **2011**, *2011*, 022. [CrossRef]
8. Arapoğlu, S.; Deliduman, C.; Ekşi, K.Y. Constraints on perturbative $f(R)$ gravity via neutron stars. *J. Cosmol. Astropart. Phys.* **2011**, *2011*, 020. [CrossRef]
9. Goswami, R.; Nzioki, A.M.; Maharaj, S.D.; Ghosh, S.G. Collapsing spherical stars in $f(R)$ gravity. *Phys. Rev. D* **2014**, *90*, 084011. [CrossRef]
10. Sharif, M.; Yousaf, Z. Electromagnetic field and dynamical instability of collapse with CDTT model. *Astropart. Phys.* **2014**, *56*, 19. [CrossRef]
11. Astashenok, A.V.; Capozziello, S.; Odintsov, S.D. Maximal neutron star mass and the resolution of the hyperon puzzle in modified gravity. *Phys. Rev. D* **2014**, *89*, 103509. [CrossRef]
12. Astashenok, A.V.; Capozziello, S.; Odintsov, S.D. Extreme neutron stars from Extended Theories of Gravity. *J. Cosmol. Astropart. Phys.* **2015**, *2015*, 001. [CrossRef]
13. Bertolami, O.; Boehmer, C.G.; Harko, T.; Lobo, F.S. Extra force in $f(R)$ modified theories of gravity. *Phys. Rev. D* **2007**, *75*, 104016. [CrossRef]
14. Harko, T.; Lobo, F.S.; Nojiri, S.I.; Odintsov, S.D. $f(R,T)$ gravity. *Phys. Rev. D* **2011**, *84*, 024020. [CrossRef]
15. Haghani, Z.; Harko, T.; Lobo, F.S.; Sepangi, H.R.; Shahidi, S. Further matters in space-time geometry: $f(R,T,R_{\mu\nu}T^{\mu\nu})$ gravity. *Phys. Rev. D* **2013**, *88*, 044023. [CrossRef]
16. Sharif, M.; Zubair, M. Energy conditions in $f(R,T,R_{\mu\nu}T^{\mu\nu})$ gravity. *J. High Energy Phys.* **2013**, *2013*, 79. [CrossRef]
17. Sharif, M.; Zubair, M. Study of thermodynamic laws in $f(R,T,R_{\mu\nu}T^{\mu\nu})$ gravity. *J. Cosmol. Astropart. Phys.* **2013**, *2013*, 042. [CrossRef]
18. Odintsov, S.D.; Sáez-Gómez, D. $f(R,T,R_{\mu\nu}T^{\mu\nu})$ gravity phenomenology and ΛCDM universe. *Phys. Lett. B* **2013**, *725*, 437. [CrossRef]
19. Ayuso, I.; Jiménez, J.B.; De la Cruz-Dombriz, A. Consistency of universally nonminimally coupled $f(R,T,R_{\mu\nu}T^{\mu\nu})$ theories. *Phys. Rev. D* **2015**, *91*, 104003. [CrossRef]
20. Baffou, E.H.; Houndjo, M.J.S.; Tosssa, J. Exploring stable models in $f(R,T,R_{\mu\nu}T^{\mu\nu})$ gravity. *Astrophys. Space Sci.* **2016**, *361*, 376. [CrossRef]
21. Sharif, M.; Waseem, A. Study of isotropic compact stars in $f(R,T,R_{\mu\nu}T^{\mu\nu})$ gravity. *Eur. Phys. J. Plus* **2016**, *131*, 1. [CrossRef]
22. Sharif, M.; Waseem, A. Physical behavior of anisotropic compact stars in $f(R,T,R_{\mu\nu}T^{\mu\nu})$ gravity. *Can. J. Phys.* **2016**, *94*, 1024. [CrossRef]
23. Yousaf, Z.; Bhatti, M.Z.; Naseer, T. Study of static charged spherical structure in $f(R,T,Q)$ gravity. *Eur. Phys. J. Plus* **2020**, *135*, 353. [CrossRef]
24. Yousaf, Z.; Bhatti, M.Z.; Naseer, T. New definition of complexity factor in $f(R,T,R_{\mu\nu}T^{\mu\nu})$ gravity. *Phys. Dark Universe* **2020**, *28*, 100535. [CrossRef]
25. Yousaf, Z.; Bhatti, M.Z.; Naseer, T. Evolution of the charged dynamical radiating spherical structures. *Ann. Phys.* **2020**, *420*, 168267. [CrossRef]
26. Yousaf, Z.; Bhatti, M.Z.; Naseer, T.; Ahmad, I. The measure of complexity in charged celestial bodies in $f(R,T,R_{\mu\nu}T^{\mu\nu})$ gravity. *Phys. Dark Universe* **2020**, *29*, 100581. [CrossRef]
27. Yousaf, Z.; Khlopov, M.Y.; Bhatti, M.Z.; Naseer, T. Influence of modification of gravity on the complexity factor of static spherical structures. *Mon. Not. R. Astron. Soc.* **2020**, *495*, 4334. [CrossRef]
28. Ovalle, J. Searching exact solutions for compact stars in braneworld: a conjecture. *Mod. Phys. Lett. A* **2008**, *23*, 3247. [CrossRef]
29. Ovalle, J.; Linares, F. Tolman IV solution in the Randall-Sundrum braneworld. *Phys. Rev. D* **2013**, *88*, 104026. [CrossRef]
30. Casadio, R.; Ovalle, J.; Da Rocha, R. The minimal geometric deformation approach extended. *Class. Quantum Grav.* **2015**, *32*, 215020. [CrossRef]
31. Ovalle, J. Decoupling gravitational sources in general relativity: from perfect to anisotropic fluids. *Phys. Rev. D* **2017**, *95*, 104019. [CrossRef]
32. Ovalle, J.; Casadio, R.; Da Rocha, R.; Sotomayor, A.; Stuchlik, Z. Black holes by gravitational decoupling. *Eur. Phys. J. C* **2018**, *78*, 1. [CrossRef]
33. Sharif, M.; Sadiq, S. Gravitational decoupled charged anisotropic spherical solutions. *Eur. Phys. J. C* **2018**, *78*, 410. [CrossRef]
34. Sharif, M.; Saba, S. Gravitational decoupled anisotropic solutions in $f(G)$ gravity. *Eur. Phys. J. C* **2018**, *78*, 921. [CrossRef]
35. Sharif, M.; Saba, S. Gravitational decoupled charged anisotropic solutions in modified Gauss-Bonnet gravity. *Chin. J. Phys.* **2019**, *59*, 481. [CrossRef]
36. Sharif, M.; Waseem, A. Anisotropic spherical solutions by gravitational decoupling in $f(R)$ gravity. *Ann. Phys.* **2019**, *405*, 14. [CrossRef]
37. Sharif, M.; Waseem, A. Effects of charge on gravitational decoupled anisotropic solutions in $f(R)$ gravity. *Chin. J. Phys.* **2019**, *60*, 426. [CrossRef]
38. Gabbanelli, L.; Rincón, Á.; Rubio, C. Gravitational decoupled anisotropies in compact stars. *Eur. Phys. J. C* **2018**, *78*, 370. [CrossRef]
39. Estrada, M.; Tello-Ortiz, F. A new family of analytical anisotropic solutions by gravitational decoupling. *Eur. Phys. J. Plus* **2018**, *133*, 1. [CrossRef]

40. Singh, K.N.; Maurya, S.K.; Jasim, M.K.; Rahaman, F. Minimally deformed anisotropic model of class one space-time by gravitational decoupling. *Eur. Phys. J. C* **2019**, *79*, 1. [CrossRef]
41. Hensh, S.; Stuchlík, Z. Anisotropic Tolman VII solution by gravitational decoupling. *Eur. Phys. J. C* **2019**, *79*, 1. [CrossRef]
42. Sharif, M.; Majid, A. Decoupled anisotropic spheres in self-interacting Brans-Dicke gravity. *Chin. J. Phys.* **2020**, *68*, 406. [CrossRef]
43. Sharif, M.; Majid, A. Extended gravitational decoupled solutions in self-interacting Brans-Dicke theory. *Phys. Dark Universe* **2020**, *30*, 100610. [CrossRef]
44. Sharif, M.; Majid, A. Effects of charge on decoupled solutions in self-interacting Brans-Dicke theory. *Phys. Dark Universe* **2021**, *32*, 100803. [CrossRef]
45. Krori, K.D.; Barua, J. A singularity-free solution for a charged fluid sphere in general relativity. *J. Phys. A Math. Gen.* **1975**, *8*, 508. [CrossRef]
46. Güver, T.; Wroblewski, P.; Camarota, L.; Özel, F. The mass and radius of the neutron star in 4U 1820–30. *Astrophys. J.* **2010**, *719*, 1807. [CrossRef]
47. Buchdahl, H.A. General relativistic fluid spheres. *Phys. Rev.* **1959**, *116*, 1027. [CrossRef]
48. Ivanov, B.V. Maximum bounds on the surface redshift of anisotropic stars. *Phys. Rev. D* **2002**, *65*, 104011. [CrossRef]
49. Herrera, L. Cracking of self-gravitating compact objects. *Phys. Lett. A* **1992**, *165*, 206. [CrossRef]
50. Heintzmann, H.; Hillebrandt, W. Neutron stars with an anisotropic equation of state-Mass, redshift and stability. *Astron. Astrophys.* **1975**, *38*, 51.
51. Hillebrandt, W.; Steinmetz, K.O. Anisotropic neutron star models-Stability against radial and nonradial pulsations. *Astron. Astrophys.* **1976**, *53*, 283.
52. Bombaci, I. The maximum mass of a neutron star. *Astron. Astrophys.* **1996**, *305*, 871.